



## Article

# Characterization and Antibacterial Activity of Silver Nanoparticles Synthesized from *Oxya chinensis sinuosa* (Grasshopper) Extract

Se-Min Kim <sup>1,2</sup>, Tai-Yong Kim <sup>1</sup>, Yun-Sang Choi <sup>3</sup> , Gyeongsik Ok <sup>1</sup> and Min-Cheol Lim <sup>1,4,\*</sup>

<sup>1</sup> Research Group of Food Safety and Distribution, Korea Food Research Institute, Wanju-gun 55365, Republic of Korea; k.semin@kfri.re.kr (S.-M.K.); k.taiyong@kfri.re.kr (T.-Y.K.); gsok@kfri.re.kr (G.O.)

<sup>2</sup> Department of Food Science and Biotechnology, Chung-Ang University, Anseong-si 17546, Republic of Korea

<sup>3</sup> Research Group of Food Processing, Korea Food Research Institute, Wanju-gun 55365, Republic of Korea; kcys0517@kfri.re.kr

<sup>4</sup> Department of Food Biotechnology, Korea University of Science and Technology, Daejeon-si 34113, Republic of Korea

\* Correspondence: mclim@kfri.re.kr; Tel.: +82-62-219-9310

**Abstract:** In this study, silver nanoparticles (AgNPs) were synthesized using a green method from an extract of the edible insect *Oxya chinensis sinuosa* (O\_extract). The formation of AgNPs (O\_AgNPs) was confirmed via UV-vis spectroscopy, and their stability was assessed using Turbiscan analysis. The size and morphology of the synthesized particles were characterized using transmission electron microscopy and field-emission scanning electron microscopy. Dynamic light scattering and zeta potential analyses further confirmed the size distribution and dispersion stability of the particles. The average particle size was  $111.8 \pm 1.5$  nm, indicating relatively high stability. The synthesized O\_AgNPs were further characterized using X-ray photoelectron spectroscopy (XPS), high-resolution X-ray diffraction (HR-XRD), and Fourier transform infrared (FTIR) spectroscopy. XPS analysis confirmed the chemical composition of the O\_AgNP surface, whereas HR-XRD confirmed its crystallinity. FTIR analysis suggested that the O\_extract plays a crucial role in the synthesis process. The antibacterial activity of the O\_AgNPs was demonstrated using a disk diffusion assay, which revealed effective activity against common foodborne pathogens, including *Salmonella* Typhimurium, *Escherichia coli*, *Staphylococcus aureus*, and *Bacillus cereus*. O\_AgNPs exhibited clear antibacterial activity, with inhibition zones of  $15.08 \pm 0.45$  mm for *S. Typhimurium*,  $15.03 \pm 0.15$  mm for *E. coli*,  $15.24 \pm 0.66$  mm for *S. aureus*, and  $13.30 \pm 0.16$  mm for *B. cereus*. These findings suggest that the O\_AgNPs synthesized from the O\_extract have potential for use as antibacterial agents against foodborne bacteria.

**Keywords:** silver nanoparticles; green synthesis; edible insects; *Oxya chinensis sinuosa*; AgNP characterization; antibacterial activity



**Citation:** Kim, S.-M.; Kim, T.-Y.; Choi, Y.-S.; Ok, G.; Lim, M.-C.

Characterization and Antibacterial Activity of Silver Nanoparticles Synthesized from *Oxya chinensis sinuosa* (Grasshopper) Extract. *Microorganisms* **2024**, *12*, 2089.

<https://doi.org/10.3390/microorganisms12102089>

Academic Editor: Peter M. Muriana

Received: 12 September 2024

Revised: 14 October 2024

Accepted: 15 October 2024

Published: 18 October 2024



**Copyright:** © 2024 by the authors. Licensee MDPI, Basel, Switzerland. This article is an open access article distributed under the terms and conditions of the Creative Commons Attribution (CC BY) license (<https://creativecommons.org/licenses/by/4.0/>).

## 1. Introduction

Foodborne illnesses remain a significant global health concern, with millions of cases reported annually. Among various causes of these illnesses, the most prevalent ones are bacterial infections resulting from contaminated foods [1]. Some foodborne bacteria can cause illness even at very low concentrations and, in severe cases, can be fatal. Contamination can occur at multiple stages, ranging from the handling of raw ingredients to packaging and distribution [2]. Therefore, preventing contamination and ensuring early detection are crucial. It is equally important to control microorganisms when the contamination levels are below the detectable threshold. This has led to growing interest in integrating antibacterial agents into food packaging materials.

Nanoparticles, defined as particles smaller than 100 nm, are emerging as promising materials for food packaging because of their unique physicochemical properties, such as

large surface area, charge, and dispersibility [3]. Among the various nanoparticles, silver nanoparticles (AgNPs) have garnered the most attention. AgNPs are used in biomedicine, agriculture, food packaging, cosmetics, catalysis, and sensors owing to their antibacterial properties [4]. Their multifunctional properties, including antibacterial, antifungal, antiviral, and antioxidant properties, make them particularly attractive for incorporation into food packaging materials [5,6]. Notably, AgNPs offer strong antibacterial activity with low toxicity to animal cells, further enhancing their potential for safe use in food applications [7–11].

Nanoparticle synthesis methods, including those for AgNPs, can be broadly classified into two approaches: top-down and bottom-up [12]. The top-down approach involves the reduction of bulk materials to nanoparticles through processes such as chemical etching, mechanical milling, laser cutting, lithography, thermal decomposition, and sputtering [13,14]. Although effective, this approach can lead to surface defects, high energy consumption, and high cost. In contrast, the bottom-up approach involves synthesizing nanoparticles from atoms using either chemical or biological methods. Chemical synthesis is widely used for metal nanoparticle production, providing precise control over particle properties. However, the chemicals involved and the by-products generated can pose risks to both human health and the environment [15]. Thus, there is a growing demand for eco-friendly reducing agents to replace traditional organic and inorganic ones. Although AgNPs are generally safe for use in human and animal cells, they pose environmental and health risks. This has spurred interest in greener biological synthesis methods that utilize bacteria, fungi, plant extracts, and polysaccharides [16,17]. Biological methods are advantageous because they avoid toxic chemicals, simplify the manufacturing process, and shorten reaction times [18]. However, challenges, such as maintaining sterile conditions and culturing cells, render microorganism-based synthesis less practical, leading to a preference for plant extracts [19]. Although plant-based syntheses have been widely studied, there is still a need to explore and develop other cost-effective and nontoxic biomaterials in addition to plants.

Amid growing environmental concerns, there is an increasing global imperative to develop eco-friendly materials. Demand for alternative proteins to reduce carbon emissions and ensure food security has increased in the food industry. Among various alternative protein sources, edible insects offer attractive solutions because of their nutritional and environmental benefits. Edible insects grow rapidly, require minimal space, and are cost-effective [20,21]. They are rich in proteins, fats, minerals, and vitamins. In Korea, seven species of edible insects are currently approved, namely, *Gryllus bimaculatus*, *Oxya chinensis sinuosa*, *Locusta migratoria*, *Tenebrio molitor* larvae, *Zophobas atratus* larvae, *Protactia brevitarsis seulensis* larvae, and *Trypoxylus dichotomus* larvae. Among these, *Oxya chinensis sinuosa* (grasshopper) has been consumed as a food for centuries and has a long history of medicinal use in Korea [22]. Dried *Oxya chinensis sinuosa* contains 3% fat, 74% protein, 18% carbohydrates, 4% ash, and various minerals, such as Ca, P, Mg, Zn, Fe, Cu, Mn, B, and Mo [23]. Previous studies have demonstrated that biomolecules, such as amino acids, vitamins, proteins, enzymes, and polysaccharides, from biological extracts can act as reducing and stabilizing agents in synthesizing AgNPs [12]. Recently, the use of insects to utilize proteins and amino acids for synthesizing AgNPs has also been reported [20–24]. These findings suggested that the abundant proteins, vitamins, and polyphenols in *Oxya chinensis sinuosa* may serve as effective catalysts for synthesizing AgNPs. As an edible insect, *Oxya chinensis sinuosa* offers a safer alternative to nonedible insects, making it a promising biomaterial for the green synthesis of AgNPs.

In this study, edible *Oxya chinensis sinuosa* was selected as a new, eco-friendly material for the synthesis of AgNPs with low toxicity to humans. The aim was to synthesize AgNPs using the entire *Oxya chinensis sinuosa*, rather than just by-products or specific parts. The synthesized AgNPs were comprehensively characterized using UV-vis spectroscopy, transmission electron microscopy (TEM), field-emission scanning electron microscopy (FE-SEM), dynamic light scattering (DLS), zeta potential analysis, X-ray photoelectron spectroscopy (XPS), high-resolution X-ray diffraction (HR-XRD), and Fourier transform

infrared (FTIR) spectroscopy. Additionally, their antibacterial activity against common foodborne pathogens was evaluated using disk diffusion assays. The findings of these analyses highlight the potential applications of the synthesized AgNPs as antibacterial agents in food packaging materials.

## 2. Materials and Methods

### 2.1. Materials

Freeze-dried powder (O\_powder) samples of *Oxya chinensis sinuosa* were obtained from a local market (Farmbang, Republic of Korea) and stored at 4 °C until the experiment. Furthermore, a 0.1 M NaOH solution to prepare an extract of *Oxya chinensis sinuosa* (O\_extract), 1 N HCl for pH adjustment, and silver nitrate were purchased from Sigma-Aldrich (St. Louis, MO, USA). Tryptic soy broth (TSB) and Tryptic soy agar (TSA) were purchased from BD Biosciences (Sparks, MD, USA) to confirm the antibacterial activity of the synthesized AgNPs. A 10 kDa MWCO centrifugal filter device (Amicon Ultra-15, Millipore, Burlington, MA, USA) was used to wash the synthesized AgNPs.

### 2.2. O\_extract Production and AgNP Synthesis

The extraction conditions were determined through preliminary experiments. Briefly, O\_powder amounts of 0.1, 0.3, and 0.5 g were tested, and the absorbance values of the AgNPs synthesized from each extract were compared to determine the optimal ratio between the insect powder and 0.1 M NaOH. Based on the method described by Jakinala et al., O\_powder (0.5 g) was mixed with 20 mL of 0.1 M NaOH solution in a vial [25]. The mixture was heated in an oven at 90 °C for 1 h with intermittent mixing every 20 min. Then, AgNPs (O\_AgNPs) were synthesized by mixing 49 mL of the pH-adjusted extract with 1 mL of 0.1 M AgNO<sub>3</sub> solution. After allowing the reaction to proceed for 48 h at room temperature, 20 mL of the supernatant was collected and filtered through a filter tube via centrifugation at 7200 × g for 10 min. The filtered O\_AgNPs were washed three times with distilled water (DW) and dispersed in DW. The synthesized O\_AgNPs were stored at 4 °C until further characterization and antibacterial activity assays were conducted.

### 2.3. UV–Vis Spectroscopy Analysis

UV–vis absorption spectra were obtained to determine the formation of AgNPs and monitor changes over the reaction time. The absorbance of the synthesized solutions was recorded over the wavelength range of 300–700 nm using a SpectraMax i3X microplate reader (Molecular Devices, Sunnyvale, CA, USA).

### 2.4. Dispersion Stability Analysis

The stability of the synthesized AgNPs was assessed using a Turbiscan Tower (Formulation, L'Union, France). The samples were placed in clear vials, and the system measured the transmittance and backscattering of near-infrared light ( $\lambda = 880$  nm) at intervals of 40  $\mu$ m from the bottom to the top of the sample. These measurements were obtained every minute over 3 h at a constant temperature of 25 °C to evaluate the stability of the dispersion.

### 2.5. TEM Analysis

The morphology and size of the AgNPs were examined using a biological transmission electron microscope (Bio-TEM, Cerritos, CA, USA) equipped with an H-7650 electron microscope (Hitachi, Tokyo, Japan) at an operating voltage of 120 kV. Samples were prepared by placing a drop of the nanoparticle solution onto a carbon 200 mesh copper grid (Ted Pella, Redding, CA, USA) and drying overnight in a desiccator before analysis using Bio-TEM.

### 2.6. FE-SEM Analysis

The morphology of the produced AgNPs was further analyzed using FE-SEM (SUPRA 40VP, Carl Zeiss, Jena, Germany) operated at 15 kV. For this analysis, each sample was drop-cast onto a silicon wafer and dried overnight in a desiccator.

### 2.7. Particle Size and Surface Charge Analysis

The particle size distribution and surface charge of the synthesized AgNPs were analyzed using DLS (Zetasizer Nano ZS90, Malvern Instruments, Malvern, UK). The particle size and zeta potential were measured at 25 °C with a wavelength of 660 nm.

### 2.8. XPS Analysis

The surface characteristics and binding energies of the synthesized AgNPs were examined using XPS. Colloidal AgNP samples were deposited onto a silicon wafer and analyzed with an AXIS Supra+ (Kratos Analytical, Stretford, UK) to determine the composition and bonding states.

### 2.9. HR-XRD Analysis

The crystallinity of the AgNPs was analyzed using HR-XRD (Empyrean, PANalytical, Houston, TX, USA) within a  $2\theta$  range of 10° to 80°, utilizing Cu K $\alpha$  radiation ( $\lambda = 0.15418$  nm) at 40 kV and 40 mA. For this analysis, the samples were drop-cast onto glass slides and dried overnight in a desiccator.

### 2.10. FTIR Analysis

FTIR analysis was used to identify the functional groups present in the synthesized AgNPs. The differences between the O\_extract and O\_AgNP samples were analyzed using an FTIR spectrometer (6300FV+IRT-5000, JASCO, Easton, MD, USA). For FTIR analysis, the washed O\_AgNPs sample was freeze-dried to obtain a powder. The powdered O\_AgNPs were then pressed into KBr pellets, and the spectra were recorded in the range of 400–4000  $\text{cm}^{-1}$ .

### 2.11. Antibacterial Activity

This study aimed to evaluate the antibacterial efficacy of the O\_AgNPs synthesized from the O\_extract against foodborne pathogens. The optimal conditions were determined through preliminary experiments based on the method described by Kim et al. [26]. Representative foodborne bacteria, including Gram-negative strains (*Salmonella* Typhimurium ATCC 14028 and *Escherichia coli* ATCC 10536) and Gram-positive strains (*Staphylococcus aureus* ATCC 25923 and *Bacillus cereus* KCTC 1094), were selected for testing. All of these strains are non-antibiotic-resistant, allowing for a clear comparison of the antibacterial activity with standard antibiotics. A disk diffusion assay was used to assess the antibacterial activity of these strains. All the bacteria were cultured overnight in 5 mL of TSB at 37 °C. Each culture was diluted to  $10^7$  CFU/mL, swabbed onto a TSA plate using a sterile cotton swab, and then dried. After drying, seven sterilized cellulose disks were placed on each plate. To accurately confirm the antibacterial activity of the O\_AgNPs, two disks of washed AgNPs were loaded onto one plate after synthesis. To confirm whether the O\_extract itself had antibacterial activity, two disks were loaded onto one plate in the same manner as the O\_AgNPs. For the comparison, DW and 1 mM AgNO<sub>3</sub> were used as negative controls. Kanamycin (30  $\mu\text{g}$ ), an antibiotic that acts on all strains, was used as a positive control. After placing 30  $\mu\text{L}$  of each sample on sterilized cellulose disks and incubating them at 37 °C for 24 h, the inhibition zone was measured.

## 3. Results and Discussion

### 3.1. Confirmation of Synthesis of AgNPs

The process of synthesizing O\_AgNPs from the O\_extract is shown in Figure 1A. The synthesis of O\_AgNPs was first confirmed visually by the color change in the reaction solution. As shown in Figure 1B, when 1 mM AgNO<sub>3</sub> was mixed with the O\_extract, the color change is due to the excitation of surface plasmon resonance in the metal particles, indicating the formation of AgNPs. The color of the solution changed from translucent to brown after the reaction. According to Krishnaraj et al., this color change is due to the excitation of surface plasmon resonance in the metal particles, indicating the formation of AgNPs [27]. UV–vis absorption spectra were measured to further verify the synthesis of AgNPs (Figure 1C). After the synthesis reaction, the

absorbance of the solution was measured in the wavelength range of 300–700 nm. Previous studies have shown that the green synthesis of AgNPs exhibits the highest absorbance peak in the range of 400–450 nm [28–30]. The UV–vis absorption spectrum of the O\_AgNPs showed a maximum peak at 408 nm, indicating the reduction in  $\text{Ag}^+$  to AgNPs ( $\text{Ag}^0$ ) [31]. To monitor the progress of the synthesis of AgNPs and the changes in absorbance over time, absorbance was measured at different time points (Figure 1C). With prolonged synthesis time, the overall absorbance increased, and the peaks became more pronounced, confirming that the AgNPs synthesized from the O\_extract were stable over time. The high dispersion stability of the synthesized O\_AgNPs was further confirmed via Turbiscan analysis, which provided additional evidence of stability along with absorbance measurements (Figure S1).

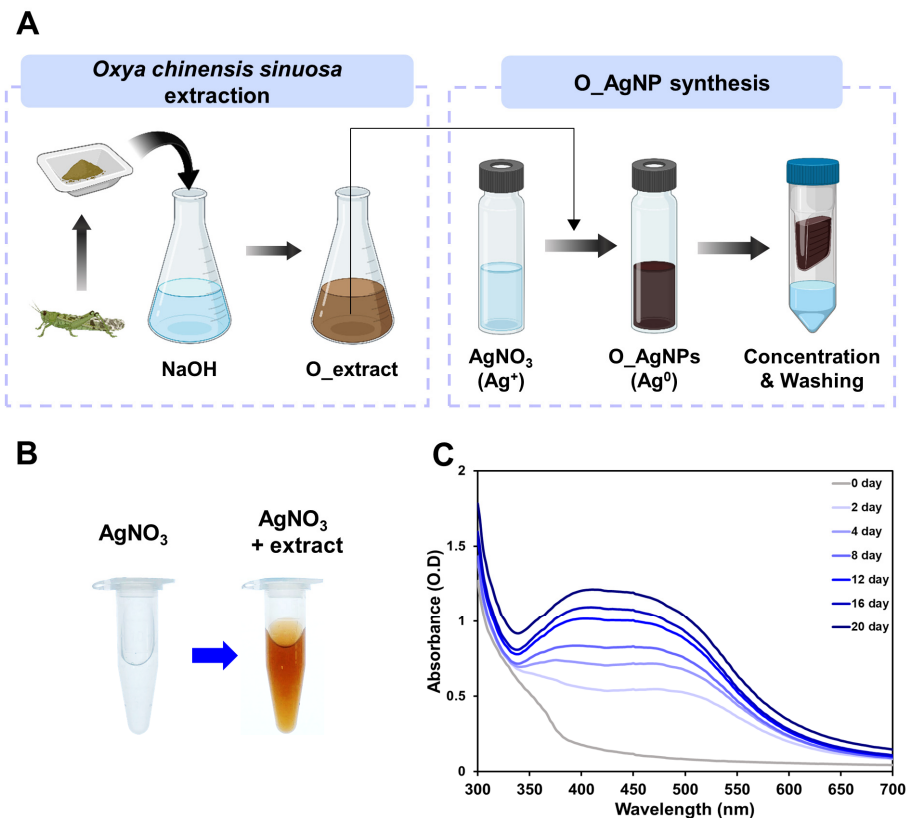


**Figure 1.** Confirmation of AgNP synthesis. (A) Schematic illustration of the synthesis process of O\_AgNPs. The figure presented was created with biorender.com. (B) Color change in the solution before and after the AgNP synthesis. (C) Time-dependent UV–vis absorption spectra for the AgNP synthesis using the O\_extract and 1 mM  $\text{AgNO}_3$  solution.

In the green synthesis of AgNPs, plant extracts are often used as reducing agents because of their steroid, saponin, carbohydrate, and flavonoid contents [32]. Previous studies have shown that *Oxya chinensis sinuosa* contains a significant number of polyphenols, which are presumed to act as reducing agents in the synthesis of AgNPs [33]. The results of the Turbiscan analysis and UV–vis measurements indicated that the AgNPs synthesized from the O\_extract exhibited significant stability over an extended period, suggesting that the O\_extract is a viable material for synthesizing AgNPs.

### 3.2. Size and Shape Analysis of Synthesized AgNPs

TEM and FE-SEM analyses were performed on the washed samples to determine the morphological characteristics of the O\_AgNPs synthesized using the O\_extract. The TEM images (Figure 2A) show that the synthesized O\_AgNPs were relatively well dispersed and exhibited small spherical shapes. The results of FE-SEM (Figure 2B) were highly consistent with those of TEM. The spherical shape is one of the defining characteristics of AgNPs that

are primarily synthesized through the green synthesis method [24,27,29]. The smaller and more evenly distributed the AgNPs produced, the larger the surface area, which facilitates higher antibacterial activity against pathogenic microorganisms [34].

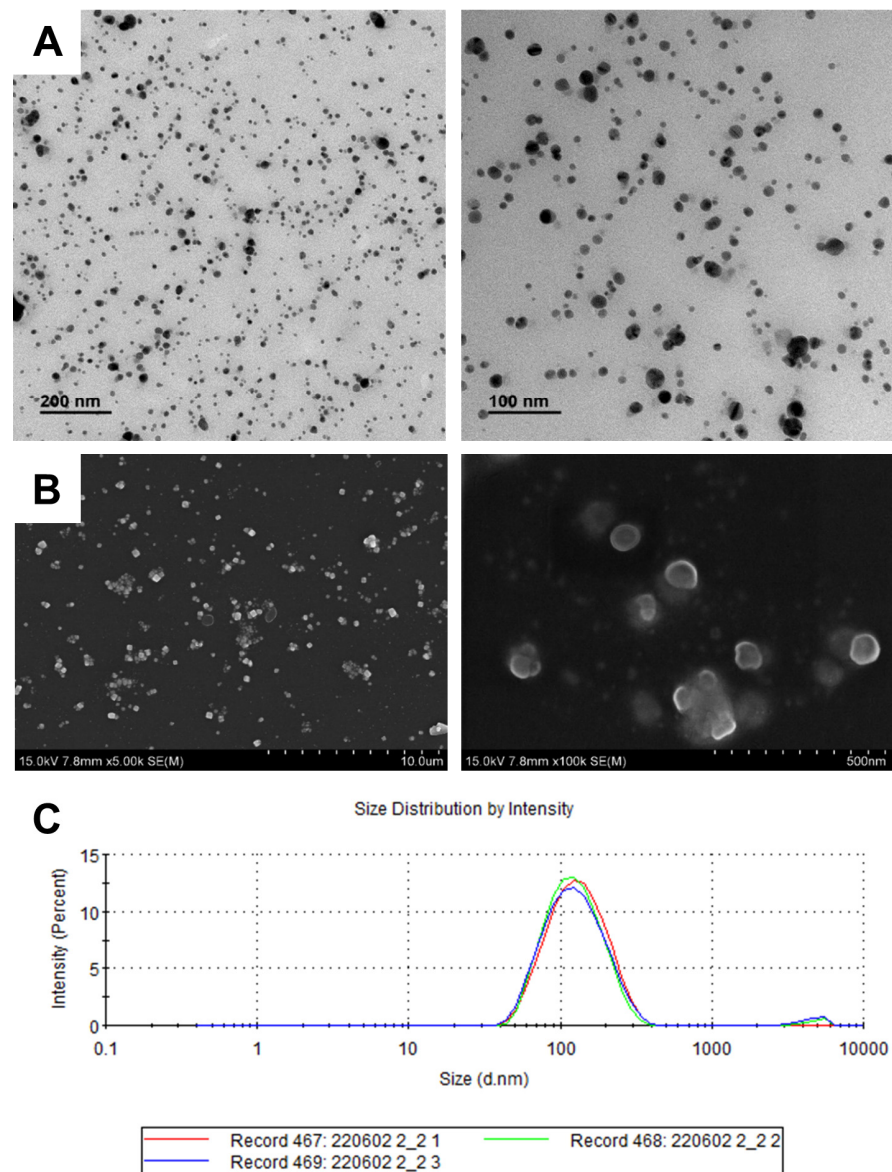


**Figure 2.** Morphological analysis of the synthesized AgNPs. (A) TEM images (different scale bars 200 nm and 100 nm); (B) size distribution of the O\_AgNPs; FE-SEM analysis of the O\_AgNPs. (Different scale bars 10 μm and 500 nm); (C) average particle size of O\_AgNPs.

The hydrodynamic size, surface zeta potential, and polydispersity index (PDI) values of the synthesized O\_AgNPs were measured via DLS. The particle characterization results for the O\_AgNPs are summarized in Table 1. The generated O\_AgNPs showed a relatively even particle size distribution, and the average particle size was approximately  $111.8 \pm 1.5$  nm (Figure 2C). The difference in the average particle sizes between the TEM/FE-SEM and DLS measurements may be attributed to the fact that TEM and FE-SEM analyze only a portion of the sample, whereas DLS considers the entire particle population. The negative zeta potential of the O\_AgNPs suggests electrostatic repulsion between particles, which contributes to the dispersion and stability of the nanoparticles in colloidal solutions [35,36]. A previous study has shown that the larger the absolute value of the zeta potential, the more stable the nanoparticles are, which helps prevent

aggregation [37]. The zeta potential of the O\_AgNPs was  $-24.1 \pm 0.9$  mV, which exceeds the threshold of 20 mV, indicating relatively high stability. The PDI indicates the particle size distribution of the O\_AgNPs, where 0 indicates a monodisperse distribution and 1 indicates a polydisperse distribution [38]. The closer the value is to 0, the less varied and more consistent is the particle size distribution. The PDI of the synthesized O\_AgNPs was 0.226, indicating a monodisperse distribution. Thus, the O\_AgNPs exhibited relatively high stability with a small size and uniform distribution, which is consistent with the results described in Section 3.1.

**Table 1.** Size and surface charge characteristics of the O\_AgNPs using DLS and zeta-potential analysis.

Source of AgNP Synthesis	Mean Size (nm)	Zeta Potential (mV)	Polydispersity Index (PDI)
O_extract	$111.8 \pm 1.5$	$-24.1 \pm 0.9$	0.226

### 3.3. Characterization of the Synthesized AgNPs

#### 3.3.1. XPS Analysis

The chemical composition of the surface of the O\_AgNPs was analyzed using XPS. Characteristic peaks were observed at each location in the XPS survey spectrum (Figure 3A). These results indicate the presence of C, O, N, and Ag on the surface of the O\_AgNPs. Figure 3B shows the XPS Ag 3d scan spectra of the O\_AgNPs. Two specific peaks at 367.7 eV and 373.4 eV were observed in the Ag 3d region. These peaks are associated with spin-orbit splitting, corresponding to the Ag 3d<sub>5/2</sub> and Ag 3d<sub>3/2</sub> core levels, respectively [39,40]. The peak difference between the Ag 3d<sub>5/2</sub> and Ag 3d<sub>3/2</sub> core levels was approximately 6 eV, indicating the presence of the Ag<sup>0</sup> state in the generated O\_AgNPs and the successful formation of AgNPs from the O\_extract [41].

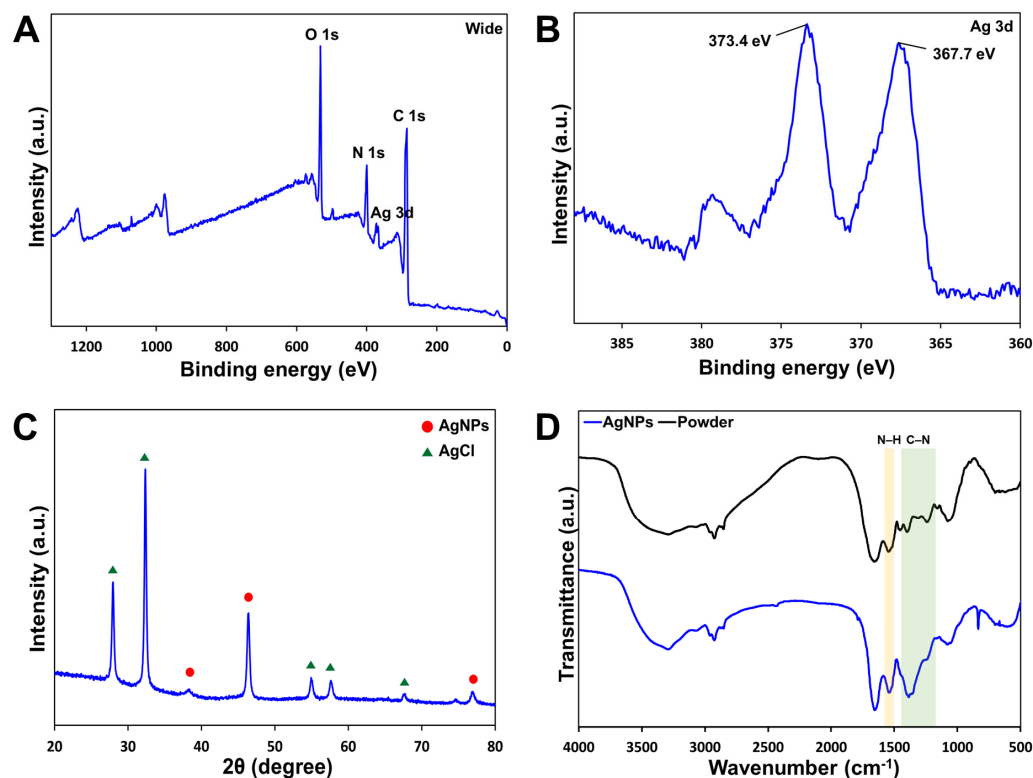


**Figure 3.** Characterization of the synthesized AgNPs. (A) XPS survey scan spectra of the O\_AgNPs; (B) XPS spectra of the Ag 3d core level of the O\_AgNPs; (C) HR-XRD pattern; (D) FTIR spectra of the O\_powder and O\_AgNPs.

### 3.3.2. HR-XRD Analysis

The crystal characteristics of the O\_AgNPs were analyzed using HR-XRD. The XRD pattern of the AgNPs synthesized using the O\_extract is shown in Figure 3C. Peaks were observed at 38.4°, 46.4°, and 77.1°, corresponding to the (111), (220), and (311) crystal planes of the AgNPs, respectively, with a face-centered cubic structure. Notably, the weak peak at 38.4° (111) correlated with the plane of the Ag crystal, indicating that the O\_AgNPs were produced in a crystalline form [42]. The additional peaks at 27.9°, 32.3°, 55.0°, 57.7°, and 67.6° correspond to the (111), (200), (311), (222), and (400) planes of AgCl, respectively [43]. This suggested the presence of chloride ions in the O\_extract, which might have led to the formation of AgCl nanoparticles [44]. Therefore, XRD analysis suggests that the O\_AgNP solution synthesized from the O\_extract may contain a mixture of crystalline AgNPs and potentially some AgCl nanoparticles.

### 3.3.3. FTIR Analysis

The functional groups of the synthesized O\_AgNPs were identified using FTIR analysis. Figure 3D shows the FTIR spectra of the O\_extract and O\_AgNPs in the spectral range of 500–4000 cm<sup>-1</sup>. The synthesized O\_AgNPs showed evident peaks at 3286 cm<sup>-1</sup>, 2933 cm<sup>-1</sup>, 2856 cm<sup>-1</sup>, 1652 cm<sup>-1</sup>, 1538 cm<sup>-1</sup>, 1384 cm<sup>-1</sup>, 1247 cm<sup>-1</sup>, 1081 cm<sup>-1</sup>, and 832 cm<sup>-1</sup>, which were confirmed to be similar to the spectrum of the O\_extract (Table 2). The peaks at 3286 cm<sup>-1</sup> (O-H stretching vibration) and 2933 cm<sup>-1</sup> (C-H stretching vibration) correspond to the aliphatic hydrocarbon groups of polyphenols, polysaccharides, and proteins bound to the AgO surface [45]. The peak at 1652 cm<sup>-1</sup> is attributed to the C=O stretching vibration. The C-H peak and C=O peak intensities increased compared with those of the O\_extract. These results suggest that both hydroxyl and carbonyl groups are involved in the reduction and stabilization of O\_AgNPs [36]. The peak at 832 cm<sup>-1</sup>, which was observed only in the O\_AgNPs, is related to the C-H stretching vibration of the alkene group, along with the peak at 2933 cm<sup>-1</sup> [46].

**Table 2.** The peaks are found in the FTIR spectra of the O\_extract and O\_AgNPs.

Wavenumber (cm <sup>-1</sup> )		Assignment
O_AgNPs	O_extract	
3286	3284	O–H stretching vibration
2933	2929	C–H stretching vibration
1652	1648	C=O stretching vibration
1538	1552	N–H bending (amide II band)
1384	1392	C–N stretching vibration
1247	1234	C–N stretching vibration (amide III band)
1081	1070	C–O stretching vibrations
832	–	C–H stretching vibration

Moreover, as indicated by the colored markers in Figure 3D, the peaks at 1538 cm<sup>-1</sup>, 1384 cm<sup>-1</sup>, and 1247 cm<sup>-1</sup> were interpreted as peaks related to amino acids. The weak peaks around 1538 cm<sup>-1</sup> and 1247 cm<sup>-1</sup> represent the amide II and III bonds between the amino acid residues present in the protein, respectively [43]. The peak at 1384 cm<sup>-1</sup> is attributed to the C–N asymmetric stretching vibration associated with the aromatic ring, and the peak at 1081 cm<sup>-1</sup> corresponds to the C–O stretching vibration [47].

By comparing the spectra of the O\_AgNPs and O\_extract, shifts and changes in the intensities of some peaks were observed. This suggests that the O\_extract is involved in the synthesis of AgNPs. When the overall spectrum was confirmed, the O\_extract was observed to contain proteins, polyphenols, and carboxylic acids and is believed to act as a stabilizing and dispersing agent during the synthesis of AgNPs.

### 3.4. Antibacterial Activity of Synthesized AgNPs

One of the most significant characteristics of AgNPs is their antibacterial activity against various bacteria [48]. The development of a green synthesis method for AgNPs is a promising approach for the control of foodborne pathogens in the food packaging industry. Accordingly, representative foodborne bacteria, including Gram-negative *S. Typhimurium* and *E. coli* and Gram-positive *S. aureus* and *B. cereus*, were selected for analysis.

The antibacterial activity of the synthesized O\_AgNPs was confirmed using the disk diffusion assay (Figure 4). For a comparison, kanamycin (30 µg), O\_extract, and 1 mM AgNO<sub>3</sub> solution were also tested on the same plate. The inhibition zones were measured as follows: *S. Typhimurium*, 15.08 ± 0.45 mm; *E. coli*, 15.03 ± 0.15 mm; *S. aureus*, 15.24 ± 0.66 mm; and *B. cereus*, 13.30 ± 0.16 mm (Table 3). Compared with kanamycin (30 µg), which was used as a positive control, the O\_AgNPs produced a clear inhibition zone, indicating significant antibacterial activity against both Gram-negative and Gram-positive bacteria.

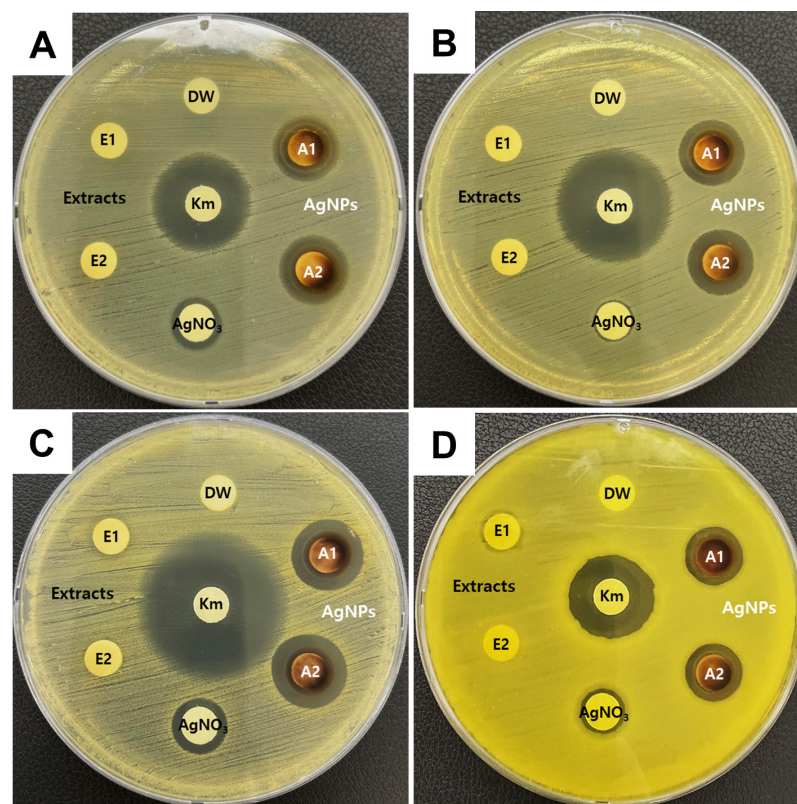


**Figure 4.** Assessment of the antibacterial activity of the O\_extract and O\_AgNPs using the disk diffusion assay. (A) *S. Typhimurium*, (B) *E. coli*, (C) *S. aureus*, and (D) *B. cereus*. Both the extract and AgNPs were tested in duplicate on a single plate. DW, distilled water; E, O\_extract; A, O\_AgNPs; Km, kanamycin.

**Table 3.** Antibacterial activity of the O\_extract and O\_AgNPs.

Sample	<i>S. Typhimurium</i>	<i>E. coli</i>	<i>S. aureus</i>	<i>B. cereus</i>
	Zone of Inhibition (mm)			
O_extract	NA	NA	NA	NA
O_AgNPs	15.08 ± 0.45	15.03 ± 0.15	15.24 ± 0.66	13.30 ± 0.16
AgNO <sub>3</sub>	12.19 ± 0.6	9.78 ± 0.43	10.81 ± 1.26	9.83 ± 0.14
Antibiotics	22.91 ± 0.13	26.45 ± 0.49	30.93 ± 0.27	18.5 ± 0.71

NA, No activity; Values represent the mean of three replicates ± SD.

The O\_extract was tested separately to confirm whether the antibacterial activity was due to the O\_extract. The absence of an inhibition zone in all four strains indicated that the O\_extract did not exhibit antibacterial activity against the selected bacteria. Additionally, a 1 mM AgNO<sub>3</sub> solution was evaluated. Although the 1 mM AgNO<sub>3</sub> solution exhibited minimal antibacterial activity, the inhibition zones for the O\_AgNPs were markedly larger across all four strains, indicating that the synthesized AgNPs had more potent antibacterial effects.

All the bacteria were cultured under identical conditions. *B. cereus* is a Gram-positive bacterium with a thick cell wall primarily composed of peptidoglycan and is known to form spores and biofilms [48]. Due to its strong defensive mechanisms against extreme conditions, it is presumed to exhibit higher resistance to antibacterial agents compared to not only Gram-negative bacteria but also other Gram-positive bacteria such as *S. aureus*. This observation is consistent with findings from previous studies [49]. Notably, the *B. cereus* strain used in this experiment consistently exhibited larger and thicker colony growth compared to other strains when cultured at the same temperature, which may have hindered the diffusion of O\_AgNPs, reducing their antibacterial activity. Among the bacteria tested, *S. aureus* showed the most pronounced sensitivity to the O\_AgNPs. The antibacterial activity of AgNPs may involve several mechanisms, such as direct interaction with the cell wall, generation of reactive oxygen species (ROS), and release of metal ions [50,51]. These mechanisms disrupt the bacterial cell wall and membrane, leading to structural deformation, leakage of intracellular contents, and DNA damage. In addition to physical effects, silver ions released from AgNPs likely contribute to the antibacterial activity. Previous studies have suggested that the antibacterial activity is due to electrostatic interactions between silver ions and bacteria [49,52]. However, the exact mechanism of the antibacterial activity caused by AgNPs remains unclear, necessitating further investigation. In conclusion, the synthesized O\_AgNPs demonstrated significant antibacterial activity against the four foodborne pathogens tested.

Many previous studies have attempted to incorporate antimicrobial AgNPs into bio-degradable and non-biodegradable polymers for food packaging and have shown effectiveness in improving food safety and shelf life [53–56]. However, human toxicity is a major hurdle for the successful introduction of AgNPs as an antipathogenic agent into food packaging. Although the probability is low, AgNPs transferred from packaging to food may accumulate and exhibit toxicity in various organs in the body [57–59]. Therefore, additional processing (coating and heat treatment) of packaging has been reported to reduce the migration of silver nanoparticles into food [60,61]; additional research is still needed to reduce human toxicity due to AgNP exposure.

#### 4. Conclusions

This study demonstrated the green synthesis of AgNPs from extracts of the edible insect *Oxya chinensis sinuosa*. The particle characteristics of the synthesized O\_AgNPs were analyzed using various characterization techniques, and their antibacterial activity against foodborne pathogens was confirmed. The synthesis was initially indicated by a color change in the O\_extract and 1 mM AgNO<sub>3</sub> reaction solution and further confirmed by the appearance of a maximum peak at 408 nm in the UV–vis absorption spectra. The increasing peak intensity over time and the results from the Turbiscan analysis suggested the high dispersion stability of the synthesized O\_AgNPs. TEM and FE-SEM analyses revealed that the O\_AgNPs were spherical and well dispersed, which is consistent with the DLS and zeta potential results. The average particle size was approximately  $111.8 \pm 1.5$  nm, with a relatively uniform size distribution. Further characterization using XPS, HR-XRD, and FTIR spectroscopy confirmed the presence of crystalline AgNPs and the role of the O\_extract in the synthesis process. The antibacterial activity of the O\_AgNPs was evaluated using a disk diffusion assay, which demonstrated their effectiveness against both Gram-positive and Gram-negative foodborne bacteria. In conclusion, this study confirmed the successful synthesis of AgNPs from the O\_extract, resulting in relatively small, spherical,

highly dispersible, and stable particles. Additionally, the synthesized O\_AgNPs exhibited significant antibacterial activity against four types of foodborne pathogens. These findings suggest that the synthesized O\_AgNPs have the potential to be used as antimicrobial agents in food packaging, although further optimization studies are required.

**Supplementary Materials:** The following supporting information can be downloaded at: <https://www.mdpi.com/article/10.3390/microorganisms12102089/s1>, Figure S1: Turbiscan of the AgNPs synthesized using the O\_extract. Backscattering profiles (%) of the O\_AgNPs.

**Author Contributions:** Conceptualization, M.-C.L. and S.-M.K.; methodology, S.-M.K., T.-Y.K., Y.-S.C. and G.O.; investigation, G.O., M.-C.L. and T.-Y.K.; data curation, Y.-S.C. and G.O.; writing—original draft preparation, S.-M.K., T.-Y.K. and M.-C.L.; writing—review and editing, S.-M.K. and M.-C.L.; visualization, S.-M.K. and Y.-S.C.; funding acquisition, Y.-S.C. and G.O. All authors have read and agreed to the published version of the manuscript.

**Funding:** This study was supported by the Main Research Program (No. ER240600-01, ER240800-01) of the Korea Food Research Institute, funded by the Ministry of Science and ICT, Republic of Korea.

**Data Availability Statement:** Data will be made available on request.

**Conflicts of Interest:** The authors declare no conflict of interest.

## References

1. Al-Hindi, R.R.; Teklemariam, A.D.; Alharbi, M.G.; Alotibi, I.; Azhari, S.A.; Qadri, I.; Alamri, T.; Harakeh, S.; Applegate, B.M.; Bhunia, A.K. Bacteriophage-based biosensors: A platform for detection of foodborne bacterial pathogens from food and environment. *Biosensors* **2022**, *12*, 905. [[CrossRef](#)] [[PubMed](#)]
2. Gao, R.; Liu, X.; Xiong, Z.; Wang, G.; Ai, L. Research progress on detection of foodborne pathogens: The more rapid and accurate answer to food safety. *Food Res. Int.* **2024**, *193*, 114767. [[CrossRef](#)] [[PubMed](#)]
3. Kumar, D.; Singh, R.; Upadhyay, S.K.; Verma, K.K.; Tripathi, R.M.; Liu, H.; Dhankher, O.P.; Tripathi, R.D.; Sahi, S.V.; Seth, C.S. Review on interactions between nanomaterials and phytohormones: Novel perspectives and opportunities for mitigating environmental challenges. *Plant Sci.* **2024**, *340*, 111964. [[CrossRef](#)]
4. Zhao, Z.Y.; Li, P.J.; Xie, R.S.; Cao, X.Y.; Su, D.L.; Shan, Y. Biosynthesis of silver nanoparticle composites based on hesperidin and pectin and their synergistic antibacterial mechanism. *Int. J. Biol. Macromol.* **2022**, *214*, 220–229. [[CrossRef](#)]
5. Majumder, S.; Huang, S.; Zhou, J.; Wang, Y.; George, S. Tannic acid-loaded halloysite clay grafted with silver nanoparticles enhanced the mechanical and antimicrobial properties of soy protein isolate films for food-packaging applications. *Food Packag. Shelf Life* **2023**, *39*, 101142. [[CrossRef](#)]
6. Raza, M.A.; Ahmad, A.; Saeed, F.; Hussain, M.; Afzaal, M.; Rasheed, A. Maize bran arabinoxylans mediated green synthesis of silver nanoparticles and their incorporation in gelatin-based packaging film. *Food Packag. Shelf Life* **2024**, *43*, 101301. [[CrossRef](#)]
7. Loo, Y.Y.; Rukayadi, Y.; Nor-Khaizura, M.A.R.; Kuan, C.H.; Chieng, B.W.; Nishibuchi, M.; Radu, S. In vitro antimicrobial activity of green synthesized silver nanoparticles against selected gram-negative foodborne pathogens. *Front. Microbiol.* **2018**, *9*, 1555. [[CrossRef](#)]
8. Yan, X.; He, B.; Liu, L.; Qu, G.; Shi, J.; Hu, L.; Jiang, G. Antibacterial mechanism of silver nanoparticles in *Pseudomonas aeruginosa*: Proteomics approach. *Metallomics* **2018**, *10*, 557–564. [[CrossRef](#)]
9. Li, W.R.; Xie, X.B.; Shi, Q.S.; Zeng, H.Y.; Ou-Yang, Y.S.; Chen, Y.B. Antibacterial activity and mechanism of silver nanoparticles on *Escherichia coli*. *Appl. Microbiol. Biotechnol.* **2010**, *85*, 1115–1122. [[CrossRef](#)]
10. Lok, C.-N.; Ho, C.-M.; Chen, R.; He, Q.-Y.; Yu, W.-Y.; Sun, H.; Tam, P.K.-H.; Chiu, J.-F.; Che, C.-M. Silver nanoparticles: Partial oxidation and antibacterial activities. *J. Biol. Inorg. Chem.* **2007**, *12*, 527–534. [[CrossRef](#)]
11. Xiu, Z.M.; Zhang, Q.B.; Puppala, H.L.; Colvin, V.L.; Alvarez, P.J.J. Negligible particle-specific antibacterial activity of silver nanoparticles. *Nano Lett.* **2012**, *12*, 4271–4275. [[CrossRef](#)] [[PubMed](#)]
12. Keat, C.L.; Aziz, A.; Eid, A.M.; Elmarzugi, N.A. Biosynthesis of nanoparticles and silver nanoparticles. *Bioresour. Bioprocess.* **2015**, *2*, 47. [[CrossRef](#)]
13. Ahmed, B.; Bilal Tahir, M.B.; Sagir, M.; Hassan, M. Bio-inspired sustainable synthesis of silver nanoparticles as next generation of nanoparticle in antimicrobial and catalytic applications. *Mater. Sci. Eng. B* **2024**, *301*, 117165. [[CrossRef](#)]
14. Ahmadi, F.; Lackner, M. Green synthesis of silver nanoparticles from *Cannabis sativa*: Properties, synthesis, mechanistic aspects, and applications. *ChemEngineering* **2024**, *8*, 64. [[CrossRef](#)]
15. Mahmoodi, N.M.; Karimi, B.; Mazarji, M.; Moghtaderi, H. Cadmium selenide quantum dot-zinc oxide composite: Synthesis, characterization, dye removal ability with UV irradiation, and antibacterial activity as a safe and high-performance photocatalyst. *J. Photochem. Photobiol. B* **2018**, *188*, 19–27. [[CrossRef](#)]

16. Chakraborty, B.; Bhat, M.P.; Basavarajappa, D.S.; Rudrappa, M.; Nayaka, S.; Kumar, R.S.; Almansour, A.I.; Perumal, K. Biosynthesis and characterization of polysaccharide-capped silver nanoparticles from *Acalypha indica* L. and evaluation of their biological activities. *Environ. Res.* **2023**, *225*, 115614. [[CrossRef](#)]
17. Zhang, X.-F.; Liu, Z.-G.; Shen, W.; Gurunathan, S. Silver nanoparticles: Synthesis, characterization, properties, applications, and therapeutic approaches. *Int. J. Mol. Sci.* **2016**, *17*, 1534. [[CrossRef](#)]
18. He, J.; Feizipour, S.; Veisi, H.; Amraii, S.A.; Zangeneh, M.M.; Hemmati, S. *Panax ginseng* root aqueous extract mediated biosynthesis of silver nanoparticles under ultrasound condition and investigation of the treatment of human lung adenocarcinoma with following the PI3K/AKT/mTOR signaling pathway. *Inorg. Chem. Commun.* **2024**, *160*, 112021. [[CrossRef](#)]
19. Ahmed, S.; Ahmad, M.; Swami, B.L.; Ikram, S. A review on plants extract mediated synthesis of silver nanoparticles for antimicrobial applications: A green expertise. *J. Adv. Res.* **2016**, *7*, 17–28. [[CrossRef](#)]
20. Mondal, A.; Maity, S.; Mondal, A.; Mondal, N.K. Antibacterial, antibiofilm and larvicidal activity of silver nanoparticles synthesized from spider silk protein. *Int. J. Biol. Macromol.* **2024**, *258*, 128775. [[CrossRef](#)]
21. Rumpold, B.A.; Schlüter, O.K. Nutritional composition and safety aspects of edible insects. *Mol. Nutr. Food Res.* **2013**, *57*, 802–823. [[CrossRef](#)]
22. Kim, W.S.; Han, J.M.; Song, H.-Y.; Byun, E.-H.; Seo, H.S.; Byun, E.-B. Edible *Oxya chinensis sinuosa*—Derived protein as a potential nutraceutical for anticancer immunity improvement. *Nutrients* **2020**, *12*, 3236. [[CrossRef](#)]
23. Kim, S.K.; Weaver, C.M.; Choi, M.K. Proximate composition and mineral content of five edible insects consumed in Korea. *CyTA J. Food* **2017**, *15*, 143–146. [[CrossRef](#)]
24. Khamhaengpol, A.; Siri, S. Fluorescent light mediated a green synthesis of silver nanoparticles using the protein extract of weaver ant larvae. *J. Photochem. Photobiol. B* **2016**, *163*, 337–344. [[CrossRef](#)]
25. Jakinala, P.; Lingampally, N.; Hameeda, B.; Sayyed, R.Z.; Khan M., Y.; Elsayed, E.A.; El Enshasy, H. Silver nanoparticles from insect wing extract: Biosynthesis and evaluation for antioxidant and antimicrobial potential. *PLoS ONE* **2021**, *16*, e0241729. [[CrossRef](#)]
26. Kim, S.-M.; Choi, H.-J.; Lim, J.-A.; Woo, M.-A.; Chang, H.-J.; Lee, N.; Lim, M.-C. Biosynthesis of silver nanoparticles from *Duchesnea indica* extracts using different solvents and their antibacterial activity. *Microorganisms* **2023**, *11*, 1539. [[CrossRef](#)]
27. Krishnaraj, C.; Jagan, E.G.; Rajasekar, S.; Selvakumar, P.; Kalaichelvan, P.T.; Mohan, N. Synthesis of silver nanoparticles using *Acalypha indica* leaf extracts and its antibacterial activity against water borne pathogens. *Colloids Surf. B Biointerfaces* **2010**, *76*, 50–56. [[CrossRef](#)]
28. Zain, M.; Nayab, S.; Rashid, Z.; Aleem, A.; Raza, H.; Yousif, M.D. Biosynthesis and in vivo wound healing abilities of *Dactyloctenium aegyptium*-mediated silver nanoparticles used as hydrogel dressing. *Process Biochem.* **2024**, *147*, 31–38. [[CrossRef](#)]
29. Shanmuganathan, R.; Brindhadevi, K.; Al-Ansari, M.M.; Al-Humaid, L.; Barathi, S.; Lee, J. In vitro investigation of silver nanoparticles synthesized using *Gracilaria verucosa*—A seaweed against multidrug resistant *Staphylococcus aureus*. *Environ. Res.* **2023**, *227*, 115782. [[CrossRef](#)]
30. He, M.; Han, Z.; Liang, Y.; Zhao, H.; Ji, X.; Ma, G.; Cui, Y.; Wang, L. Green synthesis of Ag nanoparticles using elm pod polysaccharide for catalysis and bacteriostasis. *Int. J. Biol. Macromol.* **2022**, *213*, 1078–1087. [[CrossRef](#)]
31. Singh, R.; Singh, R.; Parihar, P.; Mani, J.V. Green synthesis of silver nanoparticles using *Solanum sisymbriifolium* leaf extract: Characterization and evaluation of antioxidant, antibacterial and photocatalytic degradation activities. *Process Biochem.* **2024**, *143*, 337–352. [[CrossRef](#)]
32. Abdelghany, T.M.; Al-Rajhi, A.M.H.; Al Abboud, M.A.; Alawlaqi, M.M.; Ganash Magdah, A.; Helmy, E.A.M.; Mabrouk, A.S. Recent advances in green synthesis of silver nanoparticles and their applications: About future directions. A review. *BioNanoScience* **2018**, *8*, 5–16. [[CrossRef](#)]
33. Kim, I.W.; Markkandan, K.; Lee, J.H.; Subramaniam, S.; Yoo, S.; Park, J.; Hwang, J.S. Transcriptome profiling and in silico analysis of the antimicrobial peptides of the grasshopper *Oxya chinensis sinuosa*. *J. Microbiol. Biotechnol.* **2016**, *26*, 1863–1870. [[CrossRef](#)]
34. Rafique, M.; Sadaf, I.; Rafique, M.S.; Tahir, M.B. A review on green synthesis of silver nanoparticles and their applications. *Artif. Cells Nanomed. Biotechnol.* **2017**, *45*, 1272–1291. [[CrossRef](#)]
35. Biswas, K.; Ahamed, Z.; Dutta, T.; Mallick, B.; Khuda-Bukhsh, A.R.; Biswas, J.K.; Mandal, S.K. Green synthesis of silver nanoparticles from waste leaves of tea (*Camellia sinensis*) and their catalytic potential for degradation of azo dyes. *J. Mol. Struct.* **2024**, *1318*, 139448. [[CrossRef](#)]
36. Li, H.F.; Pan, Z.C.; Chen, J.M.; Zeng, L.X.; Xie, H.J.; Liang, Z.Q.; Wang, Y.; Zeng, N.K. Green synthesis of silver nanoparticles using *Phlebopus portentosus* polysaccharide and their antioxidant, antidiabetic, anticancer, and antimicrobial activities. *Int. J. Biol. Macromol.* **2024**, *254*, 127579. [[CrossRef](#)]
37. Yang, X.; Niu, Y.; Fan, Y.; Zheng, T.; Fan, J. Green synthesis of *Poria cocos* polysaccharides-silver nanoparticles and their applications in food packaging. *Int. J. Biol. Macromol.* **2024**, *269*, 131928. [[CrossRef](#)]
38. Khorrami, S.; Zarrabi, A.; Khaleghi, M.; Danaei, M.; Mozafari, M.R. Selective cytotoxicity of green synthesized silver nanoparticles against the MCF-7 tumor cell line and their enhanced antioxidant and antimicrobial properties. *Int. J. Nanomed.* **2018**, *13*, 8013–8024. [[CrossRef](#)]

39. Aziz, N.A.; Salleh, N.H.M.; Gopinath, S.C.B.; Kamaruddin, A.H.; Ridzuan, M.I.; Ahmad, N.A. Valorization of *Momordica charantia* seeds into phytochemically synthesized silver nanoparticles for the protection of oyster mushrooms against *Trichoderma pleuroticola*. *J. Environ. Chem. Eng.* **2023**, *11*, 111064. [[CrossRef](#)]
40. Patel, M.; Kikani, T.; Saren, U.; Thakore, S. Bactericidal, anti-biofilm, anti-oxidant potency and catalytic property of silver nanoparticles embedded into functionalised chitosan gel. *Int. J. Biol. Macromol.* **2024**, *262*, 129968. [[CrossRef](#)]
41. Teymourinia, H.; Sánchez, L.; Mollaie, F.; Ghalkhani, M.; Ramazani, A.; Hublikar, L.V.; Aminabhavi, T.M. Novel plasmonic Z-scheme-based photocatalysts and electrochemical aptasensor for the degradation and determination of epirubicin. *Chem. Eng. J.* **2024**, *480*, 148307. [[CrossRef](#)]
42. Bao, Y.; Chen, K. AgCl/Ag/g-C<sub>3</sub>N<sub>4</sub> hybrid composites: Preparation, visible light-driven photocatalytic activity and mechanism. *Nanomicro Lett.* **2016**, *8*, 182–192. [[CrossRef](#)]
43. Sarkar, J.; Naskar, A.; Nath, A.; Gangopadhyay, B.; Tarafdar, E.; Das, D.; Chakraborty, S.; Chattopadhyay, D.; Acharya, K. Innovative utilization of harvested mushroom substrate for green synthesis of silver nanoparticles: A Multi-Response optimization approach. *Environ. Res.* **2024**, *248*, 118297. [[CrossRef](#)]
44. Wasilewska, A.; Klekotka, U.; Zambrzycka, M.; Zambrowski, G.; Świącicka, I.; Kalska-Szostko, B. Physico-chemical properties and antimicrobial activity of silver nanoparticles fabricated by green synthesis. *Food Chem.* **2023**, *400*, 133960. [[CrossRef](#)]
45. Ugwoke, E.; Aisida, S.O.; Mirbahar, A.A.; Arshad, M.; Ahmad, I.; Zhao, T.K.; Ezema, F.I. Concentration induced properties of silver nanoparticles and their antibacterial study. *Surf. Interfaces* **2020**, *18*, 100419. [[CrossRef](#)]
46. Gheisari, F.; Reza Kasaei, S.; Mohamadian, P.; Chelliapan, S.; Gholizadeh, R.; Zareshahrabadi, Z.; Pooria Solhjo, S.; Vafa, E.; Mosleh-Shirazi, S.; Mohammad Amani, A.; et al. Bromelain-loaded silver nanoparticles: Formulation, characterization and biological activity. *Inorg. Chem. Commun.* **2024**, *161*, 112006. [[CrossRef](#)]
47. Li, Q.; Feng, T.; Li, H.; Wang, Z.; Wei, X.; Liu, J. Green synthesis of silver nanoparticles using endophytic bacterium *Bacillus zanthoxyli* GBE11 and their antimicrobial activity. *Biomass Convers. Bioref.* **2024**, *14*, 13173–13185. [[CrossRef](#)]
48. Granum, P.E.; Lindbäck, T. *Bacillus cereus*. In *Food Microbiology: Fundamentals and Frontiers*; Wiley: Hoboken, NJ, USA, 2012; pp. 491–502. [[CrossRef](#)]
49. Metryka, O.; Wasilkowski, D.; Dulski, M.; Adamczyk-Habrajska, M.; Augustyniak, M.; Mroziak, A. Metallic nanoparticle actions on the outer layer structure and properties of *Bacillus cereus* and *Staphylococcus epidermidis*. *Chemosphere* **2024**, *354*, 141691. [[CrossRef](#)]
50. Fan, X.; Yahia, L.; Sacher, E. Antimicrobial Properties of the Ag, Cu Nanoparticle System. *Biology* **2021**, *10*, 137. [[CrossRef](#)]
51. El-Sapagh, S.H.; El-Zawawy, N.A.; Elshobary, M.E.; Alquraishi, M.; Zabed, H.M.; Nouh, H.S. Harnessing the power of *Neobacillus niacini* AUMC-B524 for silver oxide nanoparticle synthesis: Optimization, characterization, and bioactivity exploration. *Microb. Cell Fact.* **2024**, *23*, 220. [[CrossRef](#)]
52. Kanniah, P.; Chelliah, P.; Thangapandi, J.R.; Gnanadhas, G.; Mahendran, V.; Robert, M. Green synthesis of antibacterial and cytotoxic silver nanoparticles by *Piper nigrum* seed extract and development of antibacterial silver based chitosan nanocomposite. *Int. J. Biol. Macromol.* **2021**, *189*, 18–33. [[CrossRef](#)]
53. Carbone, M.; Donia, D.T.; Sabbatella, G.; Antiochia, R. Silver nanoparticles in polymeric matrices for fresh food packaging. *J. King Saud Univ. Sci.* **2016**, *28*, 273–279. [[CrossRef](#)]
54. Li, W.; Li, L.; Zhang, H.; Yuan, M.; Qin, Y. Evaluation of PLA nanocomposite films on physicochemical and microbiological properties of refrigerated cottage cheese. *J. Food Process Preserv.* **2018**, *42*, e13362. [[CrossRef](#)]
55. Koshy, R.R.; Reghunadhan, A.; Mary, S.K.; Sadanandan, S.; Jose, S.; Thomas, S.; Pothen, L.A. AgNP anchored carbon dots and chitin nanowhisker embedded soy protein isolate films with freshness preservation for active packaging. *Food Packag. Shelf Life* **2022**, *33*, 100876. [[CrossRef](#)]
56. Trotta, F.; Da Silva, S.; Massironi, A.; Mirpoor, S.F.; Lignou, S.; Ghawi, S.K.; Charalampopoulos, D. Silver Bionanocomposites as Active Food Packaging: Recent Advances & Future Trends Tackling the Food Waste Crisis. *Polymers* **2023**, *15*, 4243. [[CrossRef](#)]
57. Nie, P.; Zhao, Y.; Xu, H. Synthesis, applications, toxicity and toxicity mechanisms of silver nanoparticles: A review. *Ecotox. Environ. Safe* **2023**, *253*, 114636. [[CrossRef](#)]
58. Gallochio, F.; Cibin, V.; Biancotto, G.; Roccato, A.; Muzzolon, O.; Carmen, L.; Simonne, B.; Manodori, L.; Fabrizi, A.; Patuzzi, I.; et al. Testing nano-silver food packaging to evaluate silver migration and food spoilage bacteria on chicken meat. *Food Addit. Contam. Part A-Chem.* **2016**, *33*, 1063–1071. [[CrossRef](#)]
59. El Mahdy, M.M.; Eldin, T.A.S.; Aly, H.S.; Mohammed, F.F.; Shaalan, M.I. Evaluation of hepatotoxic and genotoxic potential of silver nanoparticles in albino rats. *Exp. Toxicol. Pathol.* **2015**, *67*, 21–29. [[CrossRef](#)]
60. Chi, H.; Xue, J.; Zhang, C.; Chen, H.; Li, L.; Qin, Y. High Pressure Treatment for Improving Water Vapour Barrier Properties of Poly(lactic acid)/Ag Nanocomposite Films. *Polymers* **2018**, *10*, 1011. [[CrossRef](#)]
61. Aouay, M.; Aguado, R.J.; Bayés, G.; Fiol, N.; Putaux, J.L.; Boufi, S.; Delgado-Aguilar, M. In-situ synthesis and binding of silver nanoparticles to dialdehyde and carboxylated cellulose nanofibrils, and active packaging therewith. *Cellulose* **2024**, *31*, 5687–5706. [[CrossRef](#)]

**Disclaimer/Publisher's Note:** The statements, opinions and data contained in all publications are solely those of the individual author(s) and contributor(s) and not of MDPI and/or the editor(s). MDPI and/or the editor(s) disclaim responsibility for any injury to people or property resulting from any ideas, methods, instructions or products referred to in the content.